SATELLITE IMAGERY FOR MAPPING CARBON SOURCE AND SINK DISTRIBUTIONS IN CANADA'S FORESTS AND WETLANDS

by Jing M. Chen

Optical remote sensing imagery can be used to retrieve the following land surface parameters that are useful for carbon cycle modeling: (1) land cover type, (2) leaf area index, (3) fire scar age, (4) clumping index, (5) biomass, (6) wetland area, and (7) leaf pigment contents. In our regional carbon modeling, the first three parameters have been used, while progresses are being made to mapping the other parameters. In addition to these remotely sensed land surface parameters, soil texture and organic carbon maps, gridded monthly climate data from 1901 to 1998, large fire polygon data since 1959, and forest inventory data are used to produce annual spatial distributions of carbon sources and sinks in the entire Canada's forests and wetlands at 1 km resolution for the period from 1901 to 1998. The focus of this article is to review methodologies for retrieving surface parameters from remote sensing imagery and their use in modeling the carbon source and sink distribution.

To address the need to know the carbon source and sink distribution in terrestrial ecosystems for various science and policy purposes, satellite remote sensing can play a critical and indispensable role.

TABLE 1

MAJOR MODERATE-RESOLUTION OPTICAL SATELLITE SENSORS USEFUL FOR REGIONAL AND GLOBAL TERRESTRIAL CARBON ESTIMATION

Sensor Name	Abbreviation	Major Characteristics	Information Source
Advanced Alone Track Scanning Radiometer	AATSR	4 optical bands 3 thermal bands 2 view angles 1 km resolution Since 2002	http://envisat.esa.int/m-s/
Advanced Very High Resolution Radiometer	AVHRR	2 optical bands 3 thermal bands 1.1 km resolution Since 1978	http://noaasis.noaa.gov/NOAASIS/ml/avhrr.html
Global Imager	GLI	29 optical bands 7 thermal bands 0.25-1 km resolution 12/02-10/03	http://www.eoc.jaxa.jp/satellite/sendata/gli_e.html
Medium Resolution Imaging Spectrometer	MERIS	15 optical bands 300 m resolution Since 2002	http://envisat.esa.int/instruments/meris/
Moderate- Resolution Imaging Spectrometer	MODIS	20 optical bands 16 thermal bands 0.25-1 km resolution Since 1998	http://modis.gsfc.nasa.gov/
Polarization and Directionality of the Earth's Reflectances	POLDER	15 optical bands 3 polarization bands up to 14 view angles 7 km resolution 08/96-06/97, 12/02-10/03	http://smsc.cnes.fr/POLDER/
VEGETATION	VGT	4 optical bands 1.1 km resolution Since 1998	http://www.spot-vegetation.com/

INTRODUCTION

Terrestrial ecosystems have undergone changes due to direct and indirect impacts of human activities and are found to be carbon sinks in recent decades, *i.e.*, sequestering carbon from the atmosphere [1,2]. The heterogeneous nature of terrestrial ecosystems presents a major challenge in our effort to improve regional and global carbon cycle estimation, and yet the ecosystem carbon budget information not only has significance in understanding the global climate change [3,4], but has also become a major knowledge gap in formulating policies related climate change, given the options of including sinks in national greenhouse gas inventory under the Kyoto Protocol (http://unfccc.int/resource/docs/convkp/kpeng.html). Since the first polar orbiting meteorological sensor launched in 1978, *i.e.*, the Advanced Very High Resolution Radiometer (AVHRR), remote sensing from space has afforded us data for quantitative description of global land surface heterogeneities and changes, although high quality data acquired from sensors specifically designed for regional and global land surface applications only has a short history since 1998, when both VEGETATION on board SPOT 4 and the Moderate-resolution Imaging Spectrometer (MODIS) on board Terra became operational (Table 1). Although remote sensing imagery is currently insufficient in terms of the record length relative to carbon cycle time scales as well as its capability in providing key surface parameters, space-borne data nevertheless have given us indispensable information based on which much improved carbon cycle knowledge has been gained. The purpose of this article is to provide a concise review on the status of remote sensing data used for terrestrial ecosystem modeling with a main focus on the work done for Canada's forests and wetlands.

METHODS FOR BIOPHYSICAL PARAMETER RETRIEVAL

There are a number of surface parameters that can be derived from remote sensing and are useful for carbon cycle modeling (Table 2). Some of the parameters, such as land cover and LAI, are widely used in global and regional modeling and are available from many sources. Some parameters, such as clumping index, are relatively new and are only

J.M. Chen <chenj@geog.utoronto.ca>, Department of Geography, University of Toronto, 100 St. George Street, Toronto, Ontario, Canada M5S 3G3

TABLE 2

REMOTELY SENSIBLE SURFACE PARAMETERS USEFUL FOR CARBON CYCLE MODELING

Parameters	Type of satellite data	Major usages in carbon cycle modeling	Available at regional and global scale
Land cover	Multi-spectral (red, NIR and SWIR)	Differentiate between functional types	Yes
LAI	Multi-spectral (Red, NIR, SWIR)	Photosynthesis and respiration	Yes
Clumping index	Multi-angular (NIR)	Radiation distribution in canopies	Yes
Fire scar	Multi-spectral (NIR, SWIR)	Disturbance emission and forest age and regrowth	Yes
Biomass	SAR, LIDAR	Vegetation carbon stock, maintenance respiration	No
Wetland area	SAR, Optical	Aerobic and Anaerobic organic matter decomposition	No
Leaf pigments	Hyperspectral	Photosynthesis, leaf nitrogen	Yes, but preliminary

available for limited regions, while several other parameters, which are retrievable from remote sensing and critically useful for carbon cycle estimation, are not yet available for any large regions. The retrieval methodologies and the current status for each of these parameters are briefly reviewed here.

Land Cover Map

Globally, the most updated land cover map is the GLC2000 (http://www.eogeo.org/GLC2000) produced by individual countries using the SPOT4 VEGETATION data supported by the European Space Agency. The North America part of the map was jointly produced by the Canada Centre for Remote Sensing and the US Geological Survey [5] using the method of classification by progressive generalization initially developed by Cihlar *et al.* [6]. There are 35 cover types based on the Natural Vegetation Classification Standard adopted by the US Federal Geographic Data Committee. These are matched with 23 cover types in GLC2000. For carbon modeling, these cover types are grouped into several functional types, such as deciduous forest, conifer forest, grassland, cropland, tundra, barren, *etc.*, and carbon related parameter sets are assigned to these grouped cover types [7].

Leaf Area Index

Leaf area index (LAI) is defined as one half the total leaf area (all sided) per unit ground surface area [8]. This definition is suitable for both broadleaf and needleleaf forms and is now accepted by the international community [9]. There are several global LAI products that have been produced using MODIS [10], POLDER [11], MERIS [12], and VEGETATION and AATSR [13] (see Table 1 for information of these sensors). Large discrepancies are found among some of the products over Canada [14], MODIS LAI [10] being consistently 30-50% larger than VEGETATION LAI derived using an algorithm developed in Fernandes *et al.* [15]. In addition to the differences in band width and response function between the various sensors, LAI retrieval algorithms used to produce these products are also quite different, causing these large discrepancies. There are also in consistencies in LAI definition and measurement techniques and protocols. In producing and validating Canada-wide LAI products, Chen *et al.* [16] proposed a set of LAI measurement protocols as well as validation procedures, which are similar to the recent work by Abuelgasim *et al.* [14]. Through previous studies [15-19], consistent ground-based measurements of LAI were made in many forest and crop canopies over large geographical areas, providing a solid foundation for LAI map validation over Canada. For forests, it is shown that the reduced simple ratio (RSR) [20] is most significantly correlated with LAI, where RSR is defined as

$$RSR = \frac{\rho_n}{\rho_r}\left(1 - \frac{\rho_s - \rho_{min}}{\rho_{max} - \rho_{min}}\right) \qquad (1)$$

where ρ_n, ρ_r, and ρ_s are the reflectances in near infrared (NIR), red, and shortwave infrared (SWIR) bands, respectively, and ρ_{min} and ρ_{max} are the minimum and maximum reflectances in the SWIR band, determined from 1% cutoff points in the histogram of a given image. Figures 1a and 1b show the relationships between LAI and SR (i.e., ρ_n/ρ_r) and between LAI and RSR for major cover types, respectively. Compared with SR, RSR has a large sensitivity to LAI changes through suppression of the effects of the back-

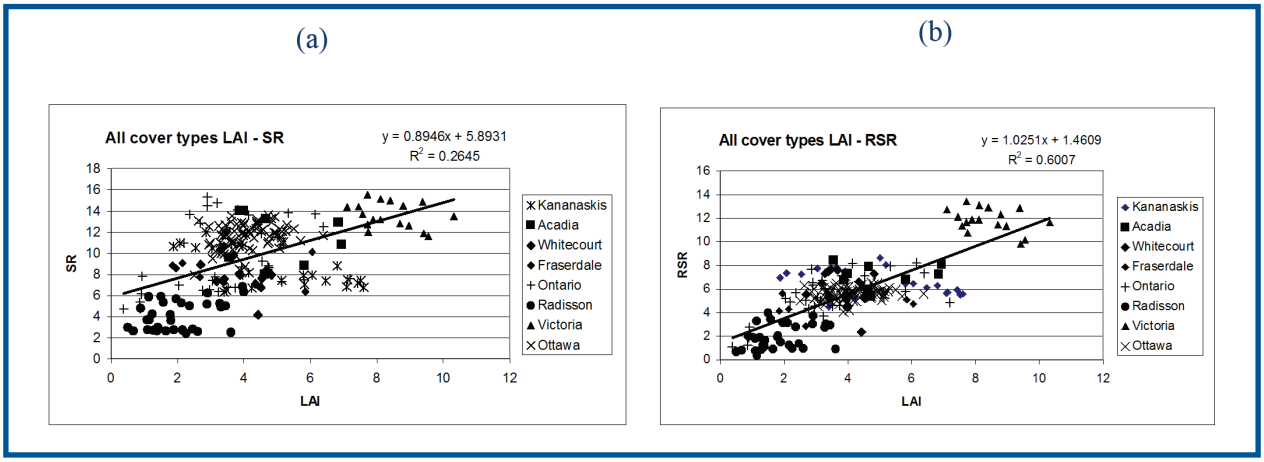

Fig. 1 Relationships between the leaf area index (LAI) and the simple ratio (SR) and between LAI and the reduced simple ratio (RSR) for all cover types in various locations in Canada, with deciduous forests and crops in Ottawa, deciduous forests in Ontario (several locations), and conifer forests in other locations [16].

ground greenness (moss and grass under forest canopy) and variability. RSR differs less for the various cover types at the same LAI than does SR, giving a clear advantage for applications to pixels of mixed cover types, which are the norm in coarse pixels because at 1 km resolution a pixel is seldom covered by only one vegetation type. This advantage is confirmed by Stenberg *et al.* [21]. Fernandes *et al.* [15] proposed an infrared simple ratio (ISR) between NIR and SWIR reflectances, showing similar sensitivities to LAI changes, however, further studies are needed to see if ISR and RSR are too sensitive to the surface water conditions and are seriously affected by rainfall events shortly prior to imaging.

Clumping Index

Nilson [22] first proposed the use of a leaf dispersion parameter to estimate the effect of nonrandom leaf spatial distributions on radiation transmission through plant canopies. The leaf distribution can either be more regular than random, or more clumped than random. Natural ecosystems generally have clumped distributions of leaves, such as groupings of leaves in shrubs and tree crowns, and this dispersion parameter is therefore often called the clumping index [17]. This clumping index is a critical input to canopy photosynthesis models with sunlit and shaded leaf stratification [23], and this stratification avoids flaws in big-leaf models, which treats a canopy as a big leaf regardless of differences in photosynthesis between sunlit and shaded leaves [24]. With the same LAI, sunlit leaves reduce and shaded leaves increase when a canopy is clumped. Chen and Cihlar [25] developed an optical instrument named TRAC (Tracing Radiation and Architecture of Canopies) to measure this clumping index based on a gap size distribution theory [26]. Measuring this clumping index has therefore become an integral part of LAI measurements, and a large dataset of clumping index for various ecosystems has been accumulated. However, as the three-dimensional canopy structure varies greatly in space, the clumping index also varies greatly, and it is highly desirable to map this index. It was not possible to do this for a large area until recently when the multi-angle POLDER data become available globally. Chen *et al.* [27] first demonstrated that the magnitude of reflectance variation from the hotspot, where the illumination and observation directions coincide, to the darkspot, where the reflectance is minimum in forward scattering direction in the principal solar plane, is mostly determined by the degree of foliage organization (clumping). Through geometrical optical simulations using the 4-Scale model [28] with a new multiple scattering scheme [29], they demonstrated that clumped canopies cast strong shadows in the forward scattering directions, reducing the darkspot reflectance. The reduction was found from data and simulations to be the largest for conifer forest, smallest for grassland, and deciduous forests are the intermediate case. They developed an angular index based on the hotspot and darkspot reflectance. These model simulations were later validated using airborne POLDER data [30] and space-borne POLDER data [24]. Through a large number of model simulations [31,32], it is shown that the normalized difference between hotspot and darkspot (NDHD) is most linearly related to the clumping index. NDHD is defined as:

$$NDHD = \frac{\rho_h - \rho_d}{\rho_h + \rho_d} \qquad (2)$$

where ρ_h and ρ_d are the hotspot and darkspot reflectance, respectively. Figure 2, shows the relationships between NDHD and the clumping index for conifer and deciduous forests separately.

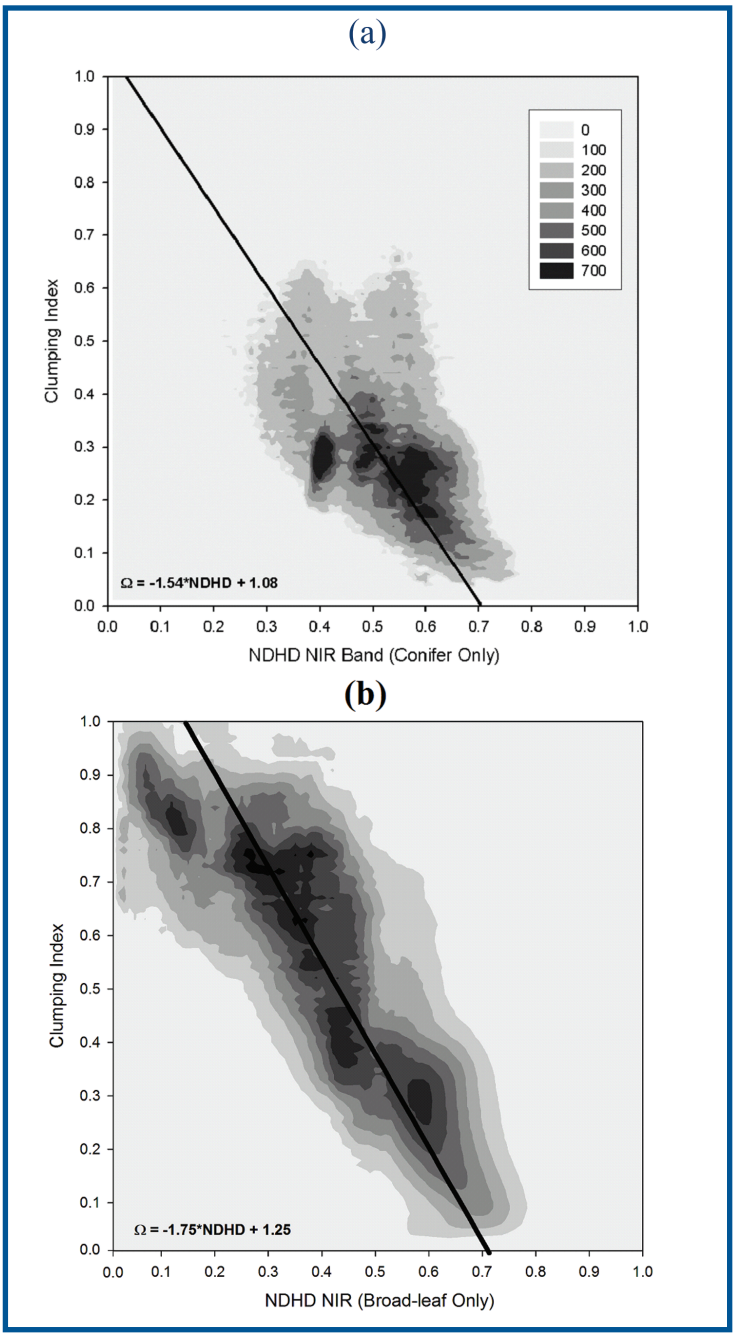

Fig.. 2 The relationship between the clumping index and the normalized difference between hotspot and darkspot (NDHD) for (a) conifer forest and (b) deciduous forests, respectively. For a random spatial distribution of leaves, the clumping index equals unity, and when foliage is clumped, it is smaller than one. The greyness indicates the number density of model results using 4-Scale with large ranges of stand structural and optical parameter inputs [31].

These modeled relationships are applied to multiple angle POLDER data for regional and global clumping index mapping [31,32]. For this purpose, POLDER data for the same pixel observed at different angles (up to 14 in one single overpass) are fitted with a simple kernel based model named FLAIR [33] or a simple exponential function [34] to find the most reliable hotspot and darkspot values for a given set of observations. Using these methodologies, Chen *et al.* [32] for the first time produced a global clumping index map using POLDER data at 7 km resolution (Figure 3). From the multiple angle views of the globe, we see that forests are most clumped (clumping index much smaller than unity) and grassland is least clumped (clumping index close to unity), and also within the same forest type, there are large variations in the index. The multiple angle view can also differentiate between the shrubland and the grassland, which are generally inseparable in a single view image. In mountainous areas, the remaining challenge is to separate the topographical effect on the angular index.

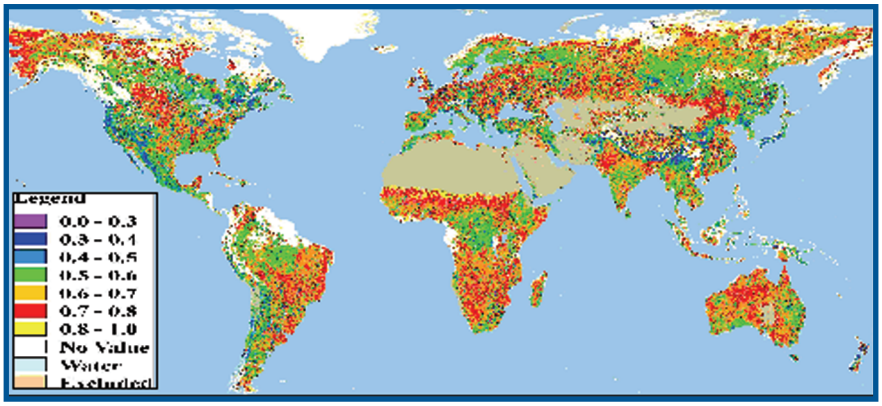

Fig. 3 **Global clumping index map produced using POLDER data at 7 km based on its relationship with an angular index, the normalized difference between hotspot and darkspot (NDHD) (Figure 2). Note that forested areas have the index considerably smaller than one, indicating high degree of foliage clumping, while grassland, cropland etc., have the index close to one [32].**

Fire Scar

Wildfires are one of the major causes of forest disturbance affecting stand dynamics, renewals, biomass and soil carbon pools, which in turn are important in forest carbon cycles [35]. Although the Large Fire Polygon Database of Canada was constructed by the Canadian Forest Service based on provincial reports [36], this database covers the periods from 1959 to 1995 and misses considerable northern fire scarring in remote areas. Remote sensing data were therefore used to fill in gaps in both space and time [37]. After a forest is burned, leaf area is greatly damaged and the standing liquid water in biomass is drastically reduced, causing the reflectance in near-infrared (NIR) to decrease and the reflectance in shortwave-infrared (SWIR) to increase. The ratio of SWIR to NIR reflectance therefore increases dramatically immediately after a fire. Figure 4, shows the variation of this ratio obtained from SPOT VEGETATION images in the summer 1998 with time since fire for a large sample of burned fire scars across Canada. The correlations are higher when separate regressions are made for individual ecoregions in Canada, r^2=0.57-80 for 16 of the 18 ecoregions [38]. As the variation in this ratio becomes small in about 25 years after the fire, fire scar dating was restricted to 25 years before the image date in 1998, with an error of ±7 years. When images acquired in multiple years are used, the accuracy in fire scar mapping and dating can be further improved [39].

Biomass

Biomass, both above and below ground, is the living carbon stock. However, so far aboveground biomass mapping for large regions has not been achieved, although it has been demonstrated that the synthetic aperture radar (SAR) can be used to retrieve biomass information, especially using not only the backscatter strength but also the coherence information [40,41]. However, regional mapping of biomass using SAR may experience variations in topography, surface dielectric constant, vegetation structure, saturation of signals at high biomass values, etc. [42], and therefore it has not yet been accomplished. Airborne light detection and ranging (LIDAR) systems have been demonstrated to be effective in retrieving forest biomass information [43,44]. Spaceborne LIDAR systems may be available in the near future [45].

Biomass is also needed in carbon cycle models to estimate the plant maintenance respiration [46]. In Canada-wide net primary productivity mapping using the Boreal Ecosystem Productivity Simulator (BEPS) [7], correlations between biomass and leaf area for two forest types (deciduous or conifer) were used. These correlations, however, can not handle variations of biomass with age at approximately the same leaf area. However, as the maintenance respiration is generally proportional to sapwood biomass rather than the total biomass [47], these crude biomass estimates may be adequate as inputs to carbon cycle models, because sapwood biomass is generally uniquely related to leaf area [48].

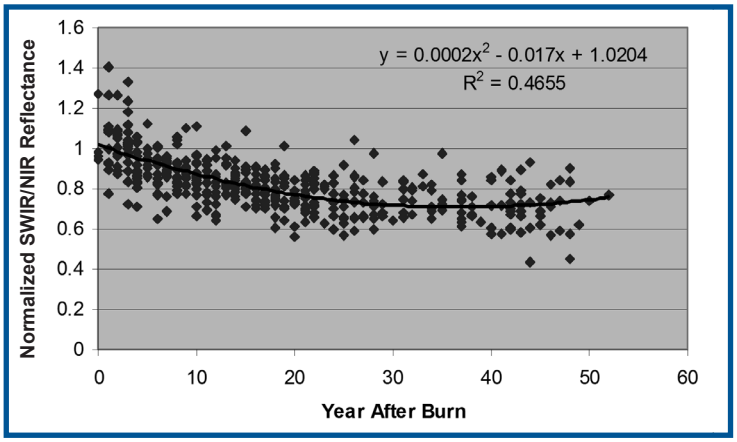

Fig. 4 **The variation of the ratio between the shortwave infrared (SWIR) reflectance and the near infrared (NIR) reflectance with the time after burn, after normalization of initial values to one. Note that the large initial decrease in the ratio and the asymptote at about 25 years after burn. Better correlations were possible by separating them into 18 ecoregions in Canada [38].**

Wetland

Wetlands have unique biogeochemical cycles involving both aerobic and anaerobic processes under fluctuating water table conditions [49]. As wetland vegetation is different from the surrounding forests and the water regime is different from the surrounding terrain, it is potentially possible to map wetland areas with both SAR (responding to water conditions) [50,51] and optical (responding to vegetation conditions) sensors [52]. However, regional mapping of wetlands suffers from variable size and shape of wetland areas as well as seasonal variation in water table affecting SAR signals. It is an area in which remote sensing techniques are underutilized.

In Canada-wide wetland carbon cycle modeling [53], wetlands are identified from drainage class information in the Soil Landscape of Canada [54]. The use of drainage class information in conjunction with topographical data allows estimation of changes in wetland water table with time, and therefore making it possible to investigate the variations of aerobic and anaerobic processes under changing climate [55].

Leaf Pigments

Leaf pigments, including chlorophyll, carotenoids and xanthophylls, absorb visible radiation and therefore affect optical remote sensing signals. Among these pigments, chlorophyll is of particular interest to carbon cycle modeling as the amount of chlorophyll per unit leaf surface area is the main control on the photosynthesis rate under given radiation and environmental conditions [56]. For natural ecosystems, the leaf chlorophyll content is closely related to the leaf nitrogen level [57,58], which is an important parameter in carbon cycle models that consider nutrient cycles [23,47]. There are leaf-level radiative transfer models that are capable of retrieving leaf pigments from leaf reflectance and/or transmittance [59,60]. Jacquemoud's leaf-level model has been applied to closed canopies for leaf chlorophyll retrieval [61]. Through combining a leaf-level model with a canopy-level model, hyperspectral remote sensing images were successfully used to retrieve leaf chlorophyll content [62]. However, reliable techniques are yet to be developed and tested for deriving leaf-level chlorophyll information for open canopies using hyperspectral remote sensing data. Using MERIS data (Table 1), some initial efforts are being made to map leaf chlorophyll globally [12], and it is expected that this parameter will be used in regional and global carbon cycle modeling in the near future.

SPATIALLY EXPLICIT CARBON CYCLE MODELING: AN EXAMPLE

Extensive research was previously done for Canada's forest carbon budgets based on forest type and age structure provided in forest inventory data [35]. In this previous study, biomass-age relationships were derived from the inventory compiled over about 100 years regardless of possible changes in growth conditions over the long period, and these relationships were applied to 457 forest types in 48 spatial units over Canada's landmass. This previous study does not include the effects of non-disturbance factors, such as the climate change, and is limited in spatial resolution (48 spatial units). The use of remote sensing not only greatly improves the spatial resolution (<1 km) but also allows estimation of changes in forest growth conditions when the past climate and current vegetation data are used in process-based modeling [37]. Figure 5 shows the major remote sensing parameters used in Canada-wide forest carbon cycle modeling as well as the major steps. One unique aspect of this modeling approach based on remote sensing is that not only non-disturbance factors (nitrogen and CO_2 fertilization effects, climate variables) are considered, as many process models do, but also disturbance factors (fire, insect, harvest) are explicitly considered. Of particular importance in modeling the disturbance effects is the forest age map in 1998 (Figure 6) created by combining forest inventory, large fire polygons, and remote sensing data for dating fire scars (Section 2.4).

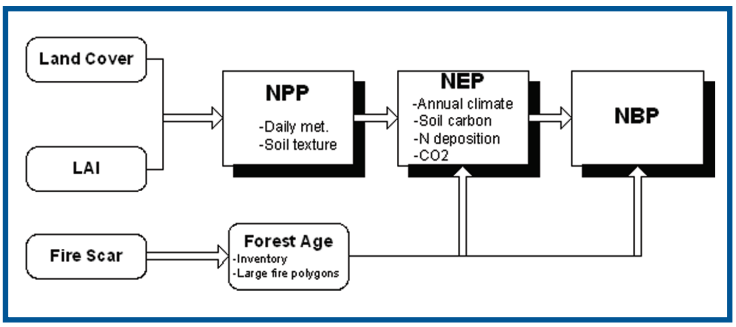

Fig. 5 An example of remote sensing products, land cover, LAI, and fire scar, used for carbon modeling for Canada's forests. The net primary productivity (NPP), which is the carbon absorption in living biomass per unit time (year) and space, is calculated in daily steps for recent years. A forest age map (Figure 6) produced from inventory, large fire polygons, and remotely sensed fire scar, is used with other inputs (climate over 100 years, soil carbon, N and CO_2) to estimate the net ecosystem productivity (NEP) and net biome productivity (NBP). NEP is NPP minus heterotrophic respiration, and NBP is NEP minus direct carbon release at the time of disturbance.

The essential information that remote sensing can provide is the quantitative surface conditions in recent years useful for spatially explicit modeling. However, the carbon cycle is a slow process, involving photosynthesis, dead organic matter accumulation and decomposition, biomass accumulation and turnover, disturbance and regrowth, *etc.*, and on average the carbon residence time is about 50 years in boreal forests [63]. In order to estimate the current carbon cycle, the spatially explicit data (including a forest age map) must be combined with historical climate records of length at least twice the residence time in order to model changes in vegetation and soil conditions over time. As the sizes of various soil carbon pools and their decomposition rates are crucial in carbon cycle estimation and are not directly available from measurements for large areas, a model spin-up approach, similar to many other ecosystem models [64], was used to estimate the pool sizes and their decomposition rates at the beginning of the modeling period at 1901 [37]. The Integrated Terrestrial Ecosystem Carbon Cycle model (InTEC) was developed to simulate disturbance and non-disturbance

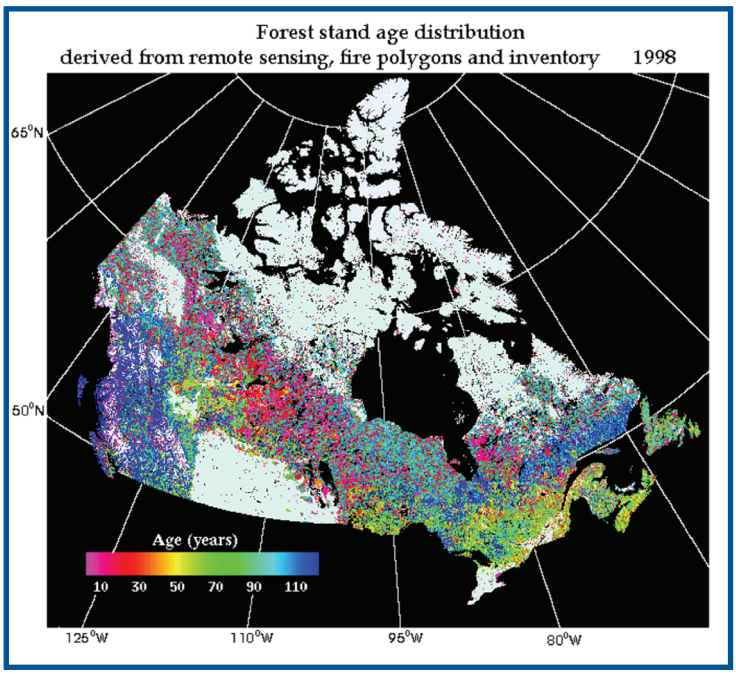

Fig. 6 Forest age map produced using forest inventory (gridded to 10 km resolution), large fire polygons (rasterized to 1 km resolution), and remote sensing imagery (1 km resolution) in 1998 for fire scar dating [37].

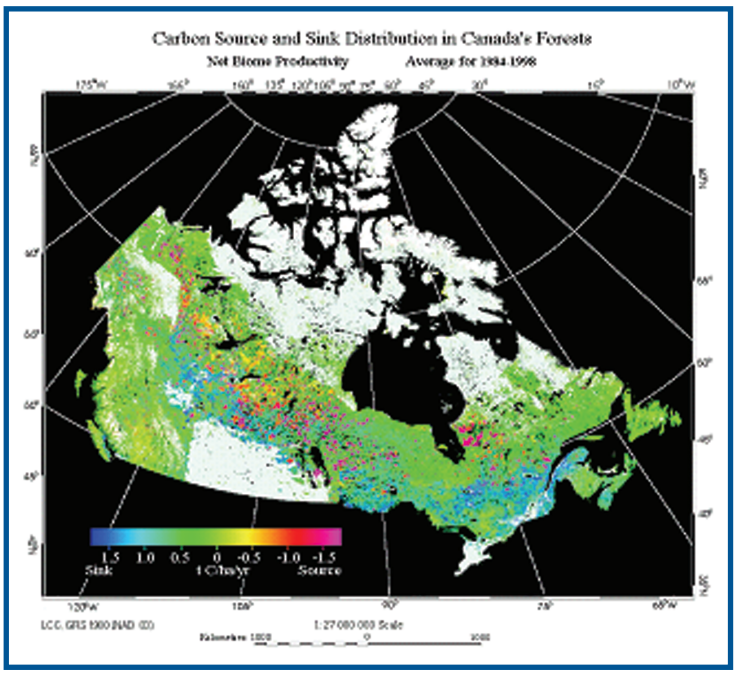

Fig. 7 Average carbon source sink distribution in Canada's forests in the period from 1984 to 1998, quantified in terms of the net biome productivity, which includes net primary productivity, heterotrophic respiration, and direct carbon release due to disturbance [37].

effects on the forest carbon cycle using these datasets [63,65]. InTEC is a combination of (i) Farqhuar's leaf-level photosynthesis model [66] applied to remote sensing pixels through a spatial and temporal scaling scheme, (ii) CENTURY soil biogeochemical model [67] modified for forest applications [65] and (iii) an empirical forest regrowth model depending on air temperature [37]. Using InTEC with inputs from remote sensing and other spatial datasets, the carbon budget of Canada's forests was calculated at 1 km resolution in annual time steps. Figure 7 shows the carbon source and sink distribution in Canada's forests averaged over the 1984-1998 period. The term, net biome productivity (NBP), is defined as net primary productivity less heterotrophic respiration (organic matter decomposition) and the direct carbon emission at the time of disturbance. When NBP is larger than zero, the surface is a sink, meaning absorbing carbon from the atmosphere, and when NBP is smaller than zero, the surface is a source. Compared with the forest age map (Figure 6), it is obvious that NBP is closely related to forest age. In BC, where most forests are older than 100 years, forests are near carbon neutral conditions because small positive effects of warming (improved nutrient cycles) and CO_2 fertilization might have offset the small decline in growth in aging forests. These results may have underestimated sinks in B.C. if the second growth forest areas are underrepresented in the forest inventory data. In prairie provinces, the overall forests are carbon sources due to frequent disturbances, and the increase in regrowth could not compensate for the dramatic increase in disturbance in 1980's and 1990's. Eastern and maritime provinces are generally carbon sinks because of large areas of productive forests gaining benefits from increased nitrogen deposition and improved nutrient conditions under warming conditions as well as a small effect of CO_2 fertilization. There is also a general gradient of decreasing sink strength from south to north because of the differential effects of warming on forests and soils. In InTEC, the decomposition of soil organic matter at higher latitudes is more sensitive to warming, while forest growth benefits less immediately from warming at higher latitudes where vegetation is sparse. Critical to modeling these spatial patterns are remotely sensed forest fire patches and forest density (LAI). Partial validations of the results of soil and vegetation carbon stocks and carbon budgets were initially made against soil carbon data in Soil Landscape of Canada, aboveground biomass data in forest inventory, and four flux tower sites [37]. Validation using more tower sites of the Fluxnet Canada Research Network was made by Ju *et al.* [55].

InTEC has recently been expanded to include aerobic and anaerobic processes in wetlands [53] and to include hydrological processes responsible for the lateral water redistribution [55] so that the total carbon absorption and release by CO_2 and CH_4 gases are also included. For these purposes, additional spatial data of the digital terrain model and drainage class are used to estimate water table and soil moisture, giving the possibility of modeling coupled water and carbon cycles.

CONCLUSIONS

Through the use of remote sensing data in combination with climate and other spatial datasets, spatially explicit carbon cycle processes in Canada's forests are simulated for the last century. The results suggest that positive effects of climate warming, nitrogen deposition, and CO_2 fertilization outweighed the negative effects of increased disturbance and

heterotrophic respiration in 1980's and 1990's, making Canada's forests a net carbon sink of about 60 MtC/y in 1980-1998. Remote sensing provided the critical spatial information to achieve this conclusion through process modeling. Active research is being conducted to consider fully the coupled water and carbon cycles and to make use of other remote sensing parameters, such as clumping index, leaf chlorophyll content, and wetland area and types.

REFERENCES

1. R.A. Houghton, "Change in the storage of terrestrial carbon since 1850", in *Soils and Global Change*, edited by R. Lal, pp. 45-64, Lewis, Boca Raton, Fla, (1995).
2. R.K. Gurney, R.M. Law, .S. Denning, P.J. Rayner, D. Baker, P. Bousquet, L. Bruhwiler, Y. Chen, P. Ciais, S. Fan, I.Y. Fung, M. Gloor, M. Heimann, K. Higuchi, J. John, T. Maki, S. Maksyutov, K. Masarie, P. Peylin, M. Prather, B.C. Pak, J. Randerson, J. Sarmiento, S. Taguchi, T. Takahashi and C. Yuen, "Towards robust regional estimates of CO_2 sources and sinks using atmospheric transport models", *Nature*, **415**, 626-630, (2002).
3. P.P. Tans, I.Y. Fung and T. Takahashi, "Observation constraints on the global atmospheric CO_2 budget", *Science*, **247**:1431-1438, (1990).
4. D.E. Pataki, J.R. Ehleringer, L.B. Flanagan, D. Yakir, D.R. Bowling, C.J. Still, N. Buchmann, J.O. Kaplan and J.A. Berry, "The application and interpretation of Keeling plots in terrestrial carbon cycle research", *Global Biogeochem. Cycles*, **17**(1), 1022, doi:10.1029/2001GB001850, (2003).
5. R. Latifovic, Z.L. Zhu, J. Cihlar, C. Giri, I. Olthof, "Land cover mapping of North and Central America-Global Land Cover 2002", *Remote Sensing of Environment*, **89**:116-127, (2004).
6. J. Cihlar, Q. Xiao, J.M. Chen, J. Beaubien, K. Fung and R. Latifovic, "Classfication by progressive generalization: a new automated methodology for remote sensing multichannel data", *International Journal of Remote Sensing*, **19**: 2685-2704, (1998).
7. J. Liu, J.M. Chen, J. Cihlar, W. Chen, "Net primary productivity mapped for Canada at 1 km resolution", *Global Ecology and Biogeography*, **11**:115-129, (2002).
8. J.M. Chen and T.A. Black, "Defining leaf area index for non-flat leaves", *Plant, Cell and Environment*, **15**:421-429, (1992).
9. I. Jonckneere, S. Fleck, K. Nackaerts, B. Muys, P. Coppin, M. Weiss, F. Baret, "Review of methods for *in situ* leaf area index determination. Part I: theries, sensors and hemisperhical photography", *Agricultural and Forest Meteorology*, **121**: 19-35, (2004).
10. R.B. Myneni, S. Hoffman, Y. Knyazikhin, J.L. Privette, J. Glassy, Y. Tian, Y. Wang, X. Song, Y. Zhang, G.R. Smith, A. Lotsch, M. Friedl, J.T. Morisette, P. Votava, R.R. Nemani, S.W. Running, "Global products of vegetation leaf area and fraction of absorbed PAR from year one of MODIS data", *Remote Sensing of Environment*, **83**, 214- 231, (2002).
11. R. Lacaze, P. Richaume, O. Hautecoeur, T. Lalanne, T.A. Quesney, F. Maignan, P. Bicheron, M. Leroy, M.F. Breon, "Advanced algorithms of ADEOS2/POLDER-2 land surface process line : application to the ADEOS-1/POLDER-1 data", *IGARSS* 2003, Toulouse, France, (2003).
12. F. Baret, J. Morissette, R. Fernandes, J.L. Champeaux, R. Myneni, J.M. Chen, S. Plummer, M. Weiss, C. Becour, and G. Derive, "Evaluation of the representativeness of networks of sites for the valiation of inter-comparison of global land biophysical products, Proposition of the CEOS-BELMANIP", *IEEE Transactions on Geiscience and Remote Sensing* (Submitted January 2005).
13. S. Plummer, A. Olivier, F. Fierens, J.M. Chen, G. Dedieu, S. Muriel, W. Cramer, C. Philippe, S. Quegan, S. Schultz and J. Hoelzemann, "The GLOBCARBON Initiative: multi-sensor estimation of global biophysical products for global terrestrial carbon studies", *ENVISAT-ERS SYMPOSIUM PROCEEDINGS*, Salzburg, Austria, 6-10 Sept 2004, European Space Agency, SP-572-ENVISAT, (2004).
14. A.A. Abuelgasim, R.A. Fernandes, and S.G. Leblanc, "DO we need regional LAI maps? Validation of global and regional coarse scale LAI maps over Canadian forests", *IEEE Transactions on Geoscience and Remote Sensing*. (in review, 2005).
15. R.A. Fernandes, C.S. Butson, G. Leblanc and R. Latifovic, "Landsat-5 and Landsat-7 ETM+ based accuracy assessment of leaf area index products for Canada derived from SPOT-4 VEGETATION data", *Canadian Journal of Remote Sensing*, **29**:241-258, (2003).
16. J.M. Chen, G. Pavlic, L. Brown, J. Cihlar, S.G. Leblanc, H.P. White, R.J. Hall, D. Peddle, D.J. King, J.A. Trofymow, E. Swift, J. Van der Sanden and P. Pellikka, "Validation of Canada-wide leaf area index maps using ground measurements and high and moderate resolution satellite imagery", *Remote Sensing of Environment*, **80**:165-184, (2002).
17. J.M. Chen, 1996. Optically-based methods for measuring seasonal variation in leaf area index of boreal conifer forests. *Agricultural and Forest Meteorology*, **80**:135-163.
18. J.M. Chen, P.M. Rich, T.S. Gower, J.M. Norman, S. Plummer, "Leaf area index of boreal forests: theory, techniques and measurements", *Journal of Geophysical Research*, **102**:29,429-29,444, (1997).
19. J.M. Chen, S.G. Leblanc, J.R. Miller, J. Freemantle, S.E. Loechel, C.L. Walthall, K.A. Innanen, H.P. White, "Compact Airborne Spectrographic Imager (CASI) used for Mapping Biophysical Parameters of Boreal Forests", *Journal of Geophysical Research-Atmosphere*, **104** (D22):27,945-27,948, (1999).
20. L.J. Brown, J.M. Chen, and S.G. Leblanc, "Short wave infrared correction to the simple ratio: an image and model analysis", *Remote Sensing of Environment*, **71**:16-25, (2000).
21. P. Stenberg, M. Rautiainen, T. Manninen, P. Voipio and H. Smolander, "Reduced simple ratio better than NDVI for estimating LAI in Finnish pine and spruce stands", *Silva Fennica*, **38**, (1):3-14, (2004).
22. T. Nilson, "A theoretical analysis of the frequency of gaps in plant stands", *Agricultural and Forest Meteorology*, **8**:25-38, (1971).
23. J.M. Chen, J. Liu, J. Cihlar and M.L. Guolden, "Daily canopy photosynthesis model through temporal and spatial scaling for remote sensing applications", *Ecological Modelling*, **124**:99-119, (1999).
24. J.M. Chen, J. Liu, S.G. Leblanc, R. Lacaze and J.-L. Roujean, "Multi-angular optical remote sensing for assessing vegetation structure and carbon absorption", *Remote Sensing of Environment*, **84**: 516-525, (2003).
25. J.M. Chen and J. Cihlar, "Plant canopy gap size analysis theory for improving optical measurements of leaf area index", *Applied Optics*, **34**:6211-6222, (1995).
26. E.E. Miller and J.M. Norman, "A sunfleck theory for plant canopies. I: lengths of sunlit segments along a transet", *Agronomy J.*, **63**: 735-738 (1971).
27. J.M. Chen, J. Liu, S.G. Leblanc, J.-L. Roujean and R. Lacaze, "Utility of Multi-angle Remote Sensing for Terrestrial Carbon Cycle Modeling", *Proceedings of the 8th International Symposium on Physical Signatures and Measurements in Remote Sensing*, Aussois, France, 8-13 January, 2001, 12 pages.
28. J.M. Chen and S. Leblanc, "A 4-scale bidirectional reflection model based on canopy architecture", *IEEE Transactions on Geoscience and Remote Sensing*. **35**:1316-1337, (1997).
29. J.M. Chen and S.G. Leblanc, "Multiple-scattering scheme useful for hyperspectral geometrical optical modelling", *IEEE Transactions on Geoscience and Remote Sensing*, **39**:1061-1071, (2001).
30. R. Lacaze, J.M. Chen, J.-L. Roujean and S.G. Leblanc, "Retrieval of vegetation clumping index using hot spot signatures measured by POLDER instrument", *Remote Sensing of Environment*, **79**: 84-95, (2002).
31. S.G. Leblanc, J.M. Chen, H.P. White and R. Latifvic, "Canada-wide foliage clumping index mapping from multi-angular POLDER measurements", *Canadian Journal of Remote Sensing* (in press, 2005).

32. J.M. Chen, C.H. Menges and S.G. Leblanc, "Global derivation of the vegetation clumping index from multi-angular satellite data", *Remote Sensing of Environment* (in press, 2005).
33. P.H. White, J.R. Miller and J.M. Chen, "Four-Scale Linear Model for Anisotropic Reflectance (FLAIR) for Plant Canopies. I: Model Description and Partial Validation", *IEEE Transactions on Geoscience and Remote Sensing*, **39**:1073-1083, (2001).
34. J.M. Chen and J. Cihlar, "A hotspot function in a simple bidirectional reflectance model for satellite applications", *Journal of Geophysical Research*, **102**:25,907-25,913, (1997).
35. W.A. Kurz and M.J. Apps, "A 70-year retrospective analysis of carbon fluxes in the Canadian forest sector", *Ecological Modelling,* **9**(2): 526-547, (1999).
36. B.D. Amiro, J.B. Todd, B.M. Wotton, K.A. Logan, M.D. Flannigan, B.J. Stock, J.A. Mason, D.L. Martell, and K.G. Hirsch, "Direct carbon emissions from Canadian forest fires, 1959-1999", *Can. J. For. Res.,* **31**: 512-525, (2001).
37. J.M. Chen, W. Ju, J. Cihlar, D. Price, J. Liu, W. Chen, J. Pan, T.A. Black and A. Barr, "Spatial distribution of carbon sources and sinks in Canada's forests based on remote sensing", *Tellus B*. **55**(2): 622-642, (2003).
38. B.D. Amiro and J.M. Chen, "Forest-fire-scar dating using SPOT-VEGETATION for Canadian ecoregions", *Canadian Journal for Forest Research*, **33**:1116-1125, (2003).
39. Q. Zhang, G. Pavlic, W. Chen, R. Latifovic, R. Fraser, J. Cihlar, "Deriving Stand Age Distribution in Boreal Forest Using SPOT VEGETATION and NOAA AVHRR Imagery", *Remote Sensing of Environment*, **91**:405-418, (2004).
40. S. Quegan, T. Le Toan, J.J. Yu, F. Ribbes, N. Floury, "Multitemporal ERS SAR analysis applied to forest mapping", *IEEE Transactions on Geoscience and Remote Sensing*, 38: 741-753, (2000).
41. K.J. Tansey, A.J. Luckman, L. Skinner, H. Balzter, T. Stozzi, W. Wagner, "Classification of forest volume resources using ERS tandem coherence and JERS backscatter data", *Remote Sensing of Environment*, **25**: 751-768, (2004).
42. T. Castel, A. Beaudoin, N. Stach, N. Stussi, T. Le Toan and P. Durand, "Sensitivity of space-borne SAR data to forest parameters over sloping terrain: Theory and experiment", *International Journal of Remote Sensing*, **22**: 2351-2376, (2001).
43. M.A. Lefsky, D. Harding, W.B. Cohen, G. Parker and H.H. Shugart, "Surface lidar remote sensing of basal area and biomass in deciduous forests of eastern Maryland, USA", *Remote Sensing of Environment*, **67**:83-98, (1999).
44. M.A. Lefsky, D.P. Turner, M. Guzy and W.B. Cohen, "Combining lidar estimates of aboveground biomass and Landsat estimates of stand age for spatially extensive validation of modeled forest productivity", *Remote Sensing of Environment*, **95**:549-558, (2005).
45. S. Hese, W. Lucht, C. Schmullius, M. Barnsley, R. Dubayah, D. Knorr, K. Newmann, T. Riedel and K. Schroter, "Global biomass mapping for an improved understanding of the CO_2 balance- the Earth observation mission Carbon –3D", *Remote Sensing of Enviroment*, **94**:94-104, (2005).
46. J.S. Amthor, J.M. Chen, J.S. Clein, S.E. Frolking, M.L. Goulden, R.F. Grant, J.S. Kimball, A.W. King, A.D. McGuire, N.T. Nikolov, C.S. Potter, S. Wang, and S.C. Wofsy, "Boreal forest CO2 exchange and evapotranspiration predicted by nine ecosystem process models: Inter-model comparisons and relations to field measurements", *J. Geophys. Res*., **106**: 33,623- 33,648, (2001).
47. R.F. Grant, Y. Zhang, F. Yuan, S. Wang, D. Gaumont-Guay, P.J. Hanson., J.M. Chen, T.A. Black, A. Barr, D.D. Baldocchi and A. Arain, "Modelling water stress effects on CO_2 and energy exchange in temperate and boreal deciduous forests", *Global Biogeochemical Cycles*, **188**:217-252 (2005).
48. S.T. Gower, J.G. Vogel, J.M. Norman, C.J. Kucharik, S.J. Steele and T.K. Stow, "Carbon distribution and aboveground net primary production in aspen, jack pine and black spruce stands in Saskatchewan and Manitoba, Canada", *Journal of Geophysical Research*, **120**:29,029-29041, (1997).
49. N.T. Roulet, "Peatlands, Carbon Storage, Greenhouse Gases and the Kyoto Protocol: Prospects and Significance for Canada", *Wetlands,* **20**: 605-615, (2000).
50. S. Arzandeh and J. Wang, "Texture evaluation of RADARSAT imagery for wetland mapping", *Canadian Journal of Remote Sensing*, **28**:653-666, (2002).
51. P.A. Townsend, "Estimating forest structure in wetlands using multitemporal SAR", *Remote Sensing of Environment*, **79**: 288-304, (2002).
52. K.S. Schmidt and A.K. Skidmore, "Spectral discrimination of vegetation types in a costal wetland", *Remote Sensing of Environment*, **85**: 92-108, (2003).
53. W. Ju and J.M. Chen, "Distribution of soil carbon stocks in Canada's forests and wetland simulated based on drainage class, topography and remote sensing:, *Hydrological Processes*, **19**:77-94, (2005).
54. C. Tarnocai, "The amount of organic carbon in various soil orders and ecological provinces in Canada", in *Soil Processes and the Carbon Cycle*, Lal, J, Kimbla, Follett, RF, Stewart, BA (eds). CRC Press: Boca Raton; 81-92, (1998).
55. W. Ju, J.M. Chen, T.A. Black, H. McCaughey and N. Roulet, "Hydrological Effects on Carbon Cycles of Canada's Forests and Wetlands", *Tellus B* (in press, 2005).
56. B.R. Bondada and J.P. Syvertsen, "Leaf chlorophyll, net gas exchange and chloroplast ultrastructure in citrus leaves of different nitrogen status", *Tree Physiology*, 23:553-559, (2003).
57. B.J. Yoder and R.E. Pettigrew-Crosby, "Predicting nitrogen and chlorophyll content and concentrations from reflectance spectra (400-2500 nm) at leaf and canopy scales", *Remote Sensing of Environment*, **53**: 199-211, (1995).
58. N. Gaborcik, "Relationship between contents of chlorophyll (a+b) (SPAS values) and nitrogen of some temperate grasses", *Photosynthetica*, **41**: 285-287, (2003).
59. S. Jacquemoud, S.L. Ustin, J. Verdebout, G. Schmuck, G. Andreoli and B. Hosgood, "Estimating leaf biochemistry using the PROSPECT leaf optical properties model", *Remote Sensing of Environment,* **56**: 194-202, (1996).
60. T.P. Dawson, J.P. Curran and S.E. Plummer, "LIBERTY - Modeling the effects of leaf biochemical concentration on reflectance spectra", *Remote Sensing of Environment*, **65**(1): 50-60, (1998).
61. P.J. Zarco-Tejada, J.R. Miller, T.L. Noland, G.H. Mohammed, P.H. Sampson, "Scaling-up and model inversion methods with narrowband optical indices for chlorophyll content estimation in closed forest canopies with hyperspectral data", *IEEE Transactions on Geoscience and Remote Sensing*, **39**(7): 1491–1507, (2001).
62. S. Jacquemoud, F.B.F.M. Danson and K. Jaggard, "Extraction of Vegetation Biophysical Parameters by Inversion of the PROSPECT + SAIL Models on Sugar Beet Canopy Reflectance Data. Application to TM and AVIRIS Sensors", *Remote Sensing of Environment*, **52**: 163-172, (1995).
63. J.M. Chen, W. Chen, J. Liu, J. Cihlar, "Annual carbon balance of Canada's forests during 1895-1996", *Global Biogeochemical Cycle*, **14** :839-850, (2000).
64. VEMAP Members, "Vegetation/Ecosystem Modeling and Analysis Project: Comparing biogeography and biogeochemistry models in continental-scale study of terrestrial ecosystem responses to climate change and CO_2 doubling", *Global Biogeochemical Cycles,* **4**: 407-437, (1995).
65. W.J. Chen, J.M. Chen, J. Liu and J. Cihlar, "Approaches for reducing uncertainties in regional forest carbon balance", *Global Biogeochemical Cycle*, **14**:827-838, (2000).
66. G.D. Farquhar, S. von Caemmerer and J.A. Berry, "A biochemical model of photosynthetic CO_2 assimilation in leaves of C_3 species", *Planta*, **149**: 78-90, (1980).
67. W.J. Parton, D.S. Ojima, C.V. Cole and D.S. Schimel, "A general model for soil organic matter dynamics: sensitivity to litter chemistry, texture amd management", *Soil Sci. Soc. Am. J.*, 147-167, (1993).